Water Research, Volume 131, 15 March 2018, pp. 151-160
DOI:10.1016/j.watres.2017.12.034

Wastewater characterisation by combining size fractionation, chemical composition and biodegradability

Kristin T. Ravndal[a,b], Eystein Opsahl[a], Andrea Bagi[a,c] and Roald Kommedal[a,*]

[a] University of Stavanger, Department of Mathematics and Natural Science, 4036 Stavanger, Norway

[b] Cranfield Water Science Institute, Cranfield University, Bedfordshire, MK43 0AL, UK

[c] Marine Environment Group, International Research Institute of Stavanger, Mekjarvik 12, 4070 Randaberg, Norway

* Corresponding author: roald.kommedal@uis.no

Submitted to Water research on 30. September 2017

Abstract

The potential for resource recovery from wastewater can be evaluated based on a detailed characterisation of wastewater. In this paper, results from fractionation and characterisation of two distinct wastewaters are reported. Using tangential flow filtration, the wastewater was fractionated into 10 size fractions ranging from 1 kDa to 1 mm, wherein the chemical composition and biodegradability were determined. Carbohydrates were dominant in particulate size fractions larger than 100 µm, indicating a potential of cellulose recovery from these fractions. While the particulate size fractions between 0.65-100 µm show a potential as a source for biofuel production due to an abundance of saturated C16 and C18 lipids. Both wastewaters were dominated by particulate (>0.65 µm), and oligo- and monomeric (<1 kDa) COD. Polymeric (1-1000 kDa) and colloidal (1000 kDa-0.65 µm) fractions had a low COD content, expected due to degradation in the sewer system upstream of the wastewater treatment plant. Biodegradation rates of particulate fractions increase with decreasing size. However, this was not seen in polymeric fractions where degradation rate was governed by chemical composition. Analytical validation of molecular weight and particle size distribution showed below filter cut-off retention of particles and polymers close to nominal cut-off, shifting the actual size distribution.

Keywords

Wastewater fractionation

Wastewater characterization

Resource recovery

Biodegradability

Abbreviations

BOD: Biological oxygen demand

COD: Chemical oxygen demand

COD/TN-ratio: COD to total nitrogen ratio

COD/TP-ratio: COD to total phosphorous ratio

MALS: Multi angle light scattering detector

OM: Organic matter

p.e: Person equivalents

PSD: Particle size distribution

SEC: Size exclusion chromatography

TSS: Total suspended solids

VSS: Volatile suspended solids

WWTP: Wastewater treatment plant

1 Introduction

Wastewater treatment has over the last century effectively improved recipient water quality, reduced water pathogenicity and improved human health (van Loosdrecht and Brdjanovic, 2014). Being primarily concerned with water and sludge quality prior to disposal, attention has been on removal mechanisms and unit processes for that purpose (Wilsenach et al., 2003). Freshwater shortage in arid regions stimulated research and development of technologies for reuse of treated wastewater (Asano and Levine, 1998). Energy and nutrient recovery has gradually been integrated with treatment, and the last decades have seen increased attention on both improved recovery and energy efficiency (Verstraete et al., 2009). More recently, wastewater is seen as an important resource for bio-based production in circular waste management (Puyol et al., 2017; Wang et al., 2015). This calls for future wastewater technologies that recover wastewater valuables, in addition to nutrient, energy and water reclamation (Puchongkawarin et al., 2015). Among putative technologies includes membrane based up-concentration (Verstraete et al., 2009), intensified and integrated distillation (Harmsen, 2007), advanced biological conversion and absorption (Matassa et al., 2015; Puyol et al., 2017) and mixed culture solvent extraction (Wahlen et al., 2011).

Characterisation of physical and chemical components in wastewater is a prerequisite for design and operation of wastewater treatment processes. Molecular and particulate size distributions of components are important for evaluation of degradation and removal mechanisms, and was first combined by Levine et al. (1991). As novel process technologies and formulation of next generation treatment objectives for resource recovery will target more specific compounds in raw wastewater, more detailed characterization is required (Choubert et al., 2013; Tran et al., 2015). Compared to current characterisation strategies (e.g. the STOWA approach; see review by Roeleveld and Van Loosdrecht, 2002), details on chemical composition and biodegradability of size classes is necessary.

Traditionally, organic matter (OM) in wastewater has been fractionated into four size fractions (Levine et al., 1991), however, the use of micro- and ultrafiltration allowed for further separation of dissolved and colloidal size fractions in later studies (Dulekgurgen et al., 2006; Karahan et al., 2008; Sophonsiri and Morgenroth, 2004). A few researchers have combined size fractionation either with chemical composition (Sophonsiri and Morgenroth, 2004) or biodegradability (Karahan et al., 2008). However, these studies do not combine all three factors. In addition, none of these studies validated the actual size distribution of the obtained fractions, a concern related to known bias effects in ultra- and nanofiltration (Cheryan, 1998). Hence, there is a need to evaluate wastewater components by the combination of a validated size fractionation, with both chemical composition and biodegradability of all size fractions.

The objectives of this study were to i) separate wastewater into several size fractions from below 1 kDa to above 1 mm and validate the size distribution of the fractions analytically, ii) quantitatively characterize the fractions in terms of nutritional and macromolecular composition, iii) determine the biodegradability and evaluate which factors affect biodegradation in each size range, and iv) evaluate the potential for resource recovery based on the detailed composition analysis performed.

2 Materials and Methods

Wastewater samples were collected from two wastewater treatment plants (WWTP) located in south-west Norway. Vik WWTP (approx. 50000 p.e.) receives wastewater from households in the Jæren region, with significant contributions from agriculture and food processing industries. Mekjarvik WWTP (approx. 250000 p.e) is located downstream of the urban areas of Stavanger and Sandnes, and receive mainly domestic wastewater with some contribution from small-scale service industries. Hence, the two wastewaters investigated here represent

(1) a high strength (especially in terms of COD) wastewater with dominant industrial loading (Vik) and (2) a typical low to intermediate strength municipal wastewater (Mekjarvik).

2.1 Wastewater sampling and fractionation

At Vik WWTP, a 50 L screened (6 mm) raw wastewater grab-sample was collected in the morning. At Mekjarvik WWTP, 60 L of wastewater was collected by a flow proportional automatic composite sampler over 20 hours (Contronics PSW 2000). Immediately upon arrival to the lab, pH of the wastewater sample was lowered to below 2.3 with concentrated hydrochloric acid and kept refrigerated at 2 °C to prevent biodegradation during storage. Size fractionation was carried out upon arrival by serial sieving, and cross flow micro- and ultrafiltration as described in the supplementary information. Sieving was performed using stainless steel sieves (VWR collection) with nominal sieve mesh sizes of 1 mm, 100 µm and 25 µm. Followed by serial microfiltration and ultrafiltration using a Cogent M1 tangential flow filtering system (Merck Millipore). Microfiltration modules used were 0.65 µm and 0.1 µm Pellicon 2 Durapore C-screen filters 0.1 m^2 (Merck Millipore), while ultrafiltration were performed using 1000 kDa, 100 kDa and 10 kDa Pellicon 2 Ultracel C-screen filter cassettes 0.1 m^2 (Merck Millipore), and 1 kDa Pellicon 2 Mini Ultrafiltration Module C-screen 0.1 m^2 (Merck Millipore).

2.2 Validation of size distribution

2.2.1 Particle size distribution

Particle size distributions (PSD) of the 100-1000 µm, 25-100 µm and 0.65-25 µm fractions were analysed by a Multisizer 4 coulter counter (Beckman Coulter) using a 1000 µm aperture tube (measuring range 25-600 µm), a 200 µm aperture tube (measurement range 4-120 µm) and a 100 µm aperture tube (2-60 µm) for the respective size fractions. For 200 and 100 µm aperture tubes, 0.9 M% NaCl was used as electrolyte, while for the largest fraction, a mixture of 0.9 M% NaCl (60 V%) and glycerol (40 V%) was used. Depending on the particle

concentration, 0.1-1 mL sample was diluted to 200 mL with corresponding electrolyte for all analysis. Electrolyte blanks were measured for background noise subtraction.

2.2.2 Molecular weight and rms-radius

Molecular weight and rms-radius distribution of polymeric and colloidal fractions were measured using an Agilent 1260 Infinity HPLC connected to multi angle light scattering (MALS) detector (Dawn Heleos II 18, Wyatt Technology) and a differential refractive index detector (Waters 2410). The HPLC system was equipped with a Shodex OHpak SB-807 HQ column, a SB-805 HQ column (with additional SB-803 HQ column for the lower fractions) and a OHpak SB-807G guard column, all kept at 20 °C throughout the experiment. Sodium azide (0.1 g L^{-1}) fixated concentrated fraction samples were filtered through either 1.2 µm or 0.45 µm cellulose nitrate syringe filters, depending on fraction size, and 100 µL was injected into an isocratic mobile phase flow of 0.5 mL min^{-1}. The mobile phase was prepared by filtering an aqueous buffer solution containing 13.4 g L^{-1} Na-HEPES (Sigma-Aldrich), 0.625 g L^{-1} HNO_3 (Sigma-Aldrich), 8.5 g L^{-1} $NaNO_3$ (Sigma-Aldrich), and 0.1 g L^{-1} sodium azide (Sigma-Aldrich) through a 0.1 µm filter (Millipore - Durapore). Sample run time was set to 90 minutes with total elution time of roughly 45 minutes, to allow re-equilibration of the columns. The injection needle was flushed between each injection to limit cross contamination. A bovine serum albumin (BSA) standard (0.5 g L^{-}, 0.185 mL g^{-1}, 66 kDa) was used as a control with regards to normalization, alignment, band broadening and for verification of the method in general. A dn/dc value of 0.165 was used as it approximate the average value for heterogeneous biopolymers (Cheong et al., 2015; Zhao et al., 2011). The ASTRA 6.0 software (Wyatt Technology, 2017) was used for data interpretation using a Berry 1st degree fit for all fractions. Detectors 8 through 18 were enabled for molecular weight analysis, while detectors 3 through 18 were enabled for the determination of rms radius of fractions larger than 100 kDa. MALS data was extrapolated at low peak-end of

fractions smaller than 10 kDa, while dRI data was extrapolated on high peak-end of fractions larger than 100 kDa.

2.3 Solids and chemical composition analysis

2.3.1 Solids

Total suspended solids (TSS) and volatile suspended solids (VSS) were determined according to standard method 2540 (APHA et al., 2012) whereby five replicates of raw wastewater samples (50 mL) were filtered with 1 µm pore size GF/C filters (Whatman). Five blank samples were prepared with 50 mL distilled water.

2.3.2 COD, nitrogen and phosphorous

Chemical oxygen demand (COD), total nitrogen (total-N), ammonium, nitrate, total phosphorous (total-P) and phosphate were determined using range appropriate commercially available spectrophotometric kits (Spectroquant, Merck). Samples were analysed in triplicates. COD, total-N, and total-P was determined in all wastewater fractions, while ammonium, nitrate, and phosphate were only measured in the TSS-filtrate and in the final permeate.

2.3.3 Carbohydrate

Carbohydrate concentration was analysed using the anthrone-sulfuric assay with recommended modifications (Leyva et al., 2008). Anthrone reagent (Sigma-Aldrich) was prepared at 0.2 % concentration in concentrated sulphuric acid (Merck Millipore). A dilution series of sucrose (5-1500 mg L^{-1}, VWR) was used as calibration standards. Samples (50 µL) were loaded onto transparent flat-bottom 96-well microtiter plates in quadruplicates before adding 200 µL Anthrone-sulphuric reagent. The contents in the loaded plate were mixed in an ultrasonic bath (10 min), followed by incubation at 95 °C (5 min) and cooling to room temperature. Absorbance was read at 485 nm ± 10 nm with a Tecan Infinite f200 PRO plate reader. Carbohydrate concentrations were transformed to COD equivalents based on an

assumed typical composition of $C_{10}H_{18}O_9$ giving 1.12 g COD g^{-1} carbohydrate (Henze et al., 2002).

2.3.4 Proteinaceous material

Total protein, in this work referred to as proteinaceous material, was determined with the NanoOrange Protein Quantitation Kit (Invitrogen N6666). A calibration standard dilution series was prepared using bovine serum albumin (>98 % heat shock fraction, Sigma-Aldrich) in Milli-Q water. The entire assay and preparative steps was performed in a darkroom with deep red illumination. Wastewater samples (10 % of total reagent volume) and reagent diluent were prepared and loaded onto transparent flat bottom 96-well microtiter plates in quadruplicates. Fluorometry was performed with a Tecan Infinite f200 PRO plate reader at excitation wavelength of 465 nm ± 20 nm and emission wavelength of 590 nm ± 10 nm. Concentrations were transformed to COD equivalents based on a typical average composition of proteinaceous material, $C_{14}H_{12}O_7N_2$, giving 1.20 g COD g^{-1} proteinaceous material (Henze et al., 2002).

2.3.5 Lipids

Lipid content was determined according to a procedure described in detail in the supplementary information. Total oils and fats were extracted in a 1:1 mixture of chloroform and methanol, and determined gravimetrically. Total lipids and fatty acids composition was determined by GC-FID (Agilent Technologies) following transesterification and methylation of lipids into fatty acid methyl esters (FAME) according to Ryckebosch et al. (2012). Total lipids and free fatty acids concentrations were transformed to COD equivalents based on a typical ThOD of 2.8 g COD g^{-1} lipid, for remaining total oils and fats a reported average of 2.03 g COD g^{-1} oils and fats was used (Henze et al., 2002).

2.4 Biodegradability

Biological oxygen demand (BOD) was measured by static respirometry (OxiTop®-C, WTW, Germany). Test samples were diluted to 200 mg COD L^{-1} final concentration for Vik wastewater, and to 100 mg COD L^{-1} for Mekjarvik wastewater. Some fractions had lower COD concentration than 100 mg COD L^{-1}, and for these fractions the highest achievable concentration based on the concentration after fractionation and upconcentration was used. Inorganic nutrients, amino acids and vitamins were added as described earlier (Bagi et al., 2014) and pH was adjusted to ~7. Three replicate test flasks were prepared for each fraction, and each flask was spiked with sludge: (1) fresh sludge (250 µL) from Vik WWTP for Vik wastewater fractions, (2) sludge (250 µL) from a fed-batch reactor (initially seeded by the same Vik sludge) maintained in our laboratory for Mekjarvik wastewater fractions. Test blanks were prepared by treating autoclaved tap water the same way as wastewater samples. Oxygen consumption was monitored for 7, 14 or 21 days at 20 °C incubation temperature under continuous mixing. Oxygen utilisation rate (OUR) was calculated as rate of change in BOD over six measurement points (gliding average). Both BOD and OUR data were normalized against initial COD concentration in the test bottles. Biodegradable and inert COD content in wastewater were estimated as described in supplementary information based on the method proposed by (Roeleveld and Van Loosdrecht, 2002).

3 Results and discussion

3.1 Wastewater composition

Wastewater composition (COD, Total-N, Total-P, carbohydrate, proteinaceous material, total oils and fats, total lipids and free fatty acids, biodegradable COD (BCOD) and inert COD) are summarised in table 1 and 2 for Vik and Mekjarvik wastewater, respectively. Overall recovery of COD was 78 ± 3 % for Vik wastewater, and 98 ± 4 % for Mekjarvik wastewater fractionations, respectively. Unidentified COD was determined as the difference between the

measured total COD and the sum of identified COD fractions. As expected from upstream sources, a higher total COD (1421 ± 58 mg COD L^{-1}) was measured in raw Vik wastewater, compared to Mekjarvik (690 ± 30 mg COD L^{-1}). Carbohydrate content as a percentage of total COD of 11.6 ± 0.8 % and 57 ± 3 % was found for Vik and Mekjarvik wastewater, respectively. Compared to measured carbohydrate content in raw municipal wastewater from earlier studies (15-36 %; Gorini et al., 2011; Huang et al., 2010; Raunkjær et al., 1994), Vik wastewater had a low carbohydrate content, while Mekjarvik wastewater contained substantially more. The total oils and fats content was 27 ± 2 % and 30 ± 2 %, with a total lipids and free fatty acids content of 21.8 ± 0.9 % and 15.4 ± 0.7 % in Vik and Mekjarvik wastewater, respectively. Lipid content were comparable to literature values (1-38 %; Gorini et al., 2011; Huang et al., 2010; Raunkjær et al., 1994), and represented 51 to 81 % of the total oils and fats. A low content of proteinaceous material was found in both Vik (0.89 ± 0.06 % of total COD) and Mekjarvik wastewater (5.8 ± 0.3 % of total COD) compared to literature values of 16-28 % (Gorini et al., 2011; Huang et al., 2010; Raunkjær et al., 1994). Vik wastewater has a high lipid concentration (table 1) which is known to interfere with the NanoOrange Protein assay (Jones et al., 2003), hence, it is not unlikely that protein content was underestimated. An underestimation of protein content could also explain the high amount of unidentified COD in Vik wastewater (61 ± 5 %).

Particle size distribution has in earlier studies been found to directly affect wastewater biodegradability (Dulekgurgen et al., 2006). The size distribution of COD, Total-N, Total-P, macromolecules, BCOD and inert COD among particulate (> 0.65 µm), colloidal (1000 kDa – 0.65 µm), polymeric (1-1000 kDa), and oligomeric and monomeric (< 1 kDa) size fractions is presented in figure 1. Relative abundance in each fraction is presented as a percentage (fraction %) of raw wastewater concentrations, except for size fractions with over 100 % recovery (table 1 and table 2). There, the sum of recovered material was used as 100 %

instead of the raw wastewater concentration in order to allow for relative comparisons. The majority of COD in Vik wastewater was found in the particulate (36 ± 2 %), and oligomeric and monomeric fractions (40 ± 2 %). In addition, 22 ± 2 % of total COD was unaccounted for during fractionation. Similarly, particulate (44 ± 2 %), and oligomeric and monomeric (53 ± 2 %) COD dominated in Mekjarvik wastewater. Low COD concentrations found in polymeric and colloidal size fractions, between 1 kDa and 0.65 µm, corresponds well with the low COD concentrations measured in polymeric size range of municipal wastewater in earlier studies (Doğruel, 2012; Dulekgurgen et al., 2006). Low COD within colloidal and polymeric ranges can be either due to degradation in the sewer system upstream of the WWTP, coagulation and flocculation of polymers and colloids, or degradation of colloids and polymers during the filtration process due to shear stress and enzymatic degradation. Degradation upstream of the WWTP would lead to: (1) an increase of bacterial biomass, which would subsequently appear as high COD in the 0.65-25 µm fraction, and (2) an increase of oligomeric and monomeric partly recalcitrant degradation products, which would appear as high inert COD in the < 1 kDa fraction. In addition, if the system has a low active biomass concentration or the biomass is predominantly flocculated or in a biofilm, depolymerisation of colloidal and polymeric COD would lead to increased concentrations of biodegradable COD in the oligomeric and monomeric size fraction (Ravndal and Kommedal, 2017). In our study, both wastewaters had high COD concentrations in these two fractions, and high concentration of inert material was found in the oligomeric and monomeric size fraction (table 1 and table 2). This suggests that significant degradation of COD in the wastewater occurred upstream of the WWTP, and that sewer system hydraulic retention may shift COD size distributions. The latter has been observed by several authors (Hvitved-Jacobsen et al., 2002).

The distribution of inert material between size fractions varied between the two studied wastewaters (table 1 and 2). Inert material was estimated by modelling the BOD data using

first order kinetics (supplementary information). Modelling BOD curves using first order kinetics generally has its limitations due to the models inability to follow complex degradation patterns. Especially for large particulate fractions with slower initial degradation and a distinct bimodal growth phase, the first order model gave a poor fit (supplementary information figure E1). However, for most fractions the first order model reached a representable ultimate BOD level, thus, a representable inert fraction could be estimated. Vik wastewater had a higher inert content in the particulate fractions (18 ± 1 %) than Mekjarvik wastewater (9 ± 1 %). Mekjarvik wastewater was highly dominated by oligomeric and monomeric inert matter (90 ± 3 %). In Vik wastewater only 32 ± 2 % of inert matter was in this fraction, however a large fraction of the inerts were not recovered. Compared to Vik WWTP, Mekjarvik WWTP has a larger inflow of petroleum industry wastewater and urban runoff. These sources contain a higher fraction of slowly biodegradable priority organic pollutants and inert pollutants (Kommedal et al., 2016). In addition, high concentrations of recalcitrant matter in the oligomeric and monomeric size fraction could be a result of degradation of OM upstream of the WWTP. Mekjarvik WWTP has a longer sewer system retention time compared to Vik WWTP, allowing for a more complete biodegradation. Finally, concentrations of inert and unknown COD in the oligomeric and monomeric fraction in Mekjarvik wastewater are comparable (table 2), further supporting the hypothesis that inert matter are due to the combination of degradation upstream of the WWTP, and urban runoff and inflow from the petroleum industry.

Both COD/TN-ratio and COD/TP-ratio decreased with decreasing size fraction for particulate and colloidal size fractions (figure 2) confirming an earlier study by van Nieuwenhuijzen et al. (2004). Hence, nitrogen and phosphorous containing substances (e.g. proteinaceous material and phospholipids) were expected to be more abundant in lower size fractions in wastewater, while macromolecules not containing nitrogen or phosphorous (e.g. cellulose,

starch and lignin) were expected to be more abundant in the large particulate fractions. This corresponds with the analysis of carbohydrates, proteinaceous material and lipids in the two wastewaters. Carbohydrates were abundant in the largest particulate fractions (figure 4), expected due to toilet paper residues (Ruiken et al., 2013). Proteinaceous material content was found to increase with decreasing size for particulate and colloidal size fractions (figure 4), and there was a significant correlation between nitrogen content and content of proteinaceous material (p-value < 0.05, SI). Total lipids and free fatty acids content increase with decreasing size in the particulate fractions (figure 4) and were positively correlated with total-P content in both wastewaters (p-value < 0.05, SI), supporting the theory of phospholipids affecting the trend seen for COD/TP-ratio.

3.2 Factors affecting biodegradation of OM in different size fractions

Maximum OUR (figure 3) and estimated first order rate constants (k_1, supplementary information table D1) increased with decreasing particle size for both Vik and Mekjarvik wastewater, for the latter the increase continued also with decreasing size for colloids. This confirms earlier results were degradation rate increased with decreasing particle size for faecal particles (Ravndal et al., 2015), egg white particles (Dimock and Morgenroth, 2006) and casein particles (Aldin et al., 2011). Increasing degradation rate with decreasing size can be explained by the particle breakup model proposed by (Dimock and Morgenroth, 2006). Surface area to volume ratio of particles increases with decreasing size, hence substrate availability will increase with decreasing size leading to a faster degradation for smaller particles. In addition, the time it took to reach maximum substrate specific OUR, was significantly higher for the two largest particle fractions of both wastewaters in comparison with the smaller size fractions (figure 3), further supporting a slower degradation of large particulate fractions.

Besides OUR and k_1, extent of degradation increased with decreasing particle size (supplementary information, figure D1). A similar increase was also observed for colloids. Extent of degradation should be the same between fractions if chemical composition was the same, hence, we interpret that as being due to a difference in chemical composition between the size fractions (table 1 and table 2). Size dependency on extent of degradation was not observed in earlier studies where extent of biodegradation was independent of particle size (Aldin et al., 2011; Ravndal et al., 2015).

Polymeric fractions on the other hand, do not show the same size dependency (figure 3). In fact, Vik wastewater polymeric fractions show the opposite trend with decreasing rate with decreasing size, however, no trend was observed for Mekjarvik wastewater. For polymers with identical chemical composition, such as dextran standards, degradation rate increase with decreasing size (Kommedal et al., 2006). The polymeric wastewater fractions differed in chemical composition (table 1 and table 2), and we suggest differences in chemical composition to be more important for biodegradation rate than differences in polymer size in the polymeric fractions.

3.3 Analytical validation of size fractionation

In earlier studies, validation of size fractionation has not been performed (Dulekgurgen et al., 2006; Karahan et al., 2008; Sophonsiri and Morgenroth, 2004). When serial filtering wastewater, actual size distribution of OM in the different size fractions can differ from the nominal membrane cut-off due to filter cake retention, induced shear stress, shape of molecules, concentration polarization and membrane rejection (Logan and Jiang, 1990). These effects result in an underestimation of low molecular weight compounds. On the contrary, induced shear stress may degrade particulate and large polymeric materials, increasing the lower molecular weight fractions. In earlier studies, such as the studies by Dulekgurgen et al. (2006) and Huang et al. (2010) this was not considered. Sophonsiri and

Morgenroth (2004) used parallel filtration when possible to overcome these problems, however, filter clogging led to the need to serially filter some samples. To minimise cake formation and concentration polarisation, and to control the mass balance and estimate recovery, serial filtration using tangential flow filtration was selected in this study. Particle size distribution (PSD), rms radius, and molecular weight distributions for Mekjarvik wastewater are presented in figure 5. Based on PSD data, the 100-1000 µm fraction contained a significant amount of particles smaller than nominal sieve cut-off (approximately 70 % of particle volume). The same was observed in the 25-100 µm fractions, but to a lesser extent (36 %). Retention of particles smaller than nominal sieve cut-off probably occurred due to filter cake retention. Observed PSD in the 0.65-25 µm fraction seem to fall well within the defined limits for the macroscopic particles (> 2 µm). However, we observed severe membrane fouling of the 0.65 µm membrane which most likely led to increased retention of colloids and polymers below the 0.65 µm nominal cut-off. Evidently, the fractions immediately below 0.65 µm had much lower COD concentrations (table 1 and 2). In spite of this, chemical composition and biodegradability of the immediately lower size fractions are expected to be representative due to non-selective retention. Cumulative weight average molecular weight and particle diameter of colloidal and polymeric size fractions (figure 5) show a decrease in diameter or molecular weight with descending nominal filter cut-off, however, molecules and particles larger than membrane cut-off was present. For polymeric fractions, a larger shift towards higher size fractions was seen for size fractions with decreasing molecular weight. This could be an effect of the shape of the molecules, or alternatively, a result of overrepresentation of larger molecules in the MALS technique, since bigger molecules scatter light exponentially more than small ones (Wyatt, 1993).

3.4 Implications for wastewater treatment processes and resource recovery

Detailed analysis of wastewater composition is a prerequisite for potential resource recovery from wastewater. Size distributions are important for development and selection of adequate unit processes, and both elemental and macromolecular information are necessary for proper recovery estimations with respect to the aforementioned unit processes. In addition, both design and operation of novel and complex recovery plants would benefit greatly from the use of advanced bioprocess models able to predict and systematically analyse system performance. Compared to the existing modelling frameworks used in the field (ASM and ADM models), this would probably mean higher model resolution (several fractional state variables), and several stoichiometric and kinetic parameters. Consequently, compositional analysis as presented in this work is required, both in terms of size fractionation and chemical species composition. By combining particle size distribution, chemical composition, and biodegradability analysis, an example of such an analysis is given of two wastewaters representing two very different scenarios for recovery: The classical household and diverse industrial and the food-industrial dominated municipal wastewaters. In both wastewaters, the two largest particulate fractions (> 1 mm and 100 µm – 1 mm) contained mainly carbohydrates (table 1 and table 2), likely due to toilet paper residuals. Earlier research has shown that sieving raw wastewater with 0.35 mm has great potential to recover slowly biodegradable cellulose from toilet paper, recovered cellulose could be used as feedstock for biofuel production or for production of new toilet paper (Ruiken et al., 2013). Based on the results of this study sieves down to 0.1 mm might be applicable for extraction of cellulose from raw wastewater. Removing the large particulate fraction mainly composed of slowly degradable carbohydrates early, could lead to more efficient biological treatment stages downstream of the sieves.

The particulate size fractions between 0.65-100 µm has a high lipids content in both wastewaters. The reason for this is unclear, however, in the dairy dominated Vik wastewater we suspect this to be lipid micelles from milk fat, and presence of general fat globules (both known to be in the lower µm range; Fox and McSweeney, 2006). The most abundant lipids in these size fraction were C16 (relative concentration 38 % in Vik wastewater and 31 % in Mekjarvik wastewater, SI) and C18 lipids (relative concentration 43 % in Vik wastewater and 54 % in Mekjarvik wastewater, SI). In addition, a high saturation levels of C16 and C18 was found in both wastewaters (combined saturation level of 62 % in Vik wastewater and 58 % in Mekjarvik wastewater, SI). Abundance of highly saturated C16 and C18 lipids is ideal for biodiesel production (Zhu et al., 2017), hence, the two size fractions between 0.65-100 µm are appropriate fractions for direct biofuel recovery.

Enhanced energy recovery by biogas production and treatment process energy efficiency are both dependent on the ability of wastewater treatment unit processes to separate COD containing components before bacterial oxidation (Sutton et al., 2011). This is a key argument used for anaerobic wastewater treatment, however, residual effluent COD and lack of nutrient removal mechanisms limit its use as stand-alone processes. Another strategy is to maximize separation of COD containing components from the raw wastewater upstream of bioconversion processes by enhanced primary treatment (Verstraete et al., 2009). Our results indicate that the particulate fraction that normally do not settle in the primary settler, the 0.65 – 25 µm fraction contain 15-22 % of the raw COD (almost all biodegradable), would upon adequate separation significantly enhance energy performance and recovery. Furthermore, the high lipid content in this fraction would stimulate biogas production potential, as the specific COD of lipids are high. Contrary to energy, nutrient recovery potential in the particulate fractions are limited. About 80 % of the size class specific nutrients are found in the low M_W dissolved fraction (> 1 kDa), and unit operations for direct recovery should focus on these.

While this paper focus on wastewater characterization and potential for resource recovery, recovery also rely on the technological and economic feasibility. Ruiken et al. (2013) presented an economic and technical evaluation of cellulose recovery from municipal wastewater, and concluded sieving of the > 350 µm fraction to be a feasible energy recovery and efficiency measure. Lipids recovery, as highlighted here as a potential resource, has been technically and economically evaluated using algal bioreactors, but full-scale implementation is still a challenge due to unfeasible technical or economical limitations (Zhu et al, 2017). Of the several challenges summarized, efficient and economically favourable extraction and purification unit processes needs to be developed for wastewater lipids recovery.

4 Conclusions

We investigated biodegradability, COD and nutrient composition on detailed size fractionated wastewaters. To our knowledge, this is the most detailed and comprehensive compositional analysis published and allow for novel strategies for modelling and resource recovery. Key findings are:

- Particulate size fractions larger than 100 µm are highly abundant in carbohydrates, possibly from toilet paper, that can be recovered by sieving. The particulate size fractions between 0.65-100 µm are highly abundant in highly saturated C16 and C18 lipids, making these size fractions a good source for lipids extraction for biodiesel production.
- Biodegradation rates of particles in wastewater were controlled by particle size, i.e., surface area to volume ratio of the organic matter, resulting in smaller particles having higher degradation rates. In the polymeric fraction, degradation rates of soluble polymeric organic matter were governed by chemical composition and not by polymer size.

- The two municipal wastewaters analysed here were dominated by particulate and oligomeric and monomeric size organic matter. Very little COD was found in polymeric and colloidal fractions, possibly due to degradation in the sewer upstream from WWTP.
- Overall recovery of organic material was relatively high in both fractionation experiments. Analytical validation of actual PSD in our size-fractions showed below filter cut-off retention of particles close to nominal cut-off in particulate size ranges, leading to PSD shifting to lower sizes. An opposite trend was observed for polymeric fractions, where a shift towards higher than the nominal membrane pore sizes was seen.

5 Acknowledgements

The authors want to thank Leif Ydstebø at IVAR for providing wastewater and valuable discussion on results for this research. Institut des sciences analytiques et de physico-chimie pour l'environnement et les Matériaux, L'Equipe de Physique et Chimie des Polymères at the university of Pau, France, with researchers Buno Grassl, Stephanie Reynaud, and Laurent Rodriguez for use of equipment, hosting and providing training for co-author Eystein Opsahl for the SEC-MALS analysis.

6 References

Aldin, S., Nakhla, G., Ray, M.B., 2011. Modeling the influence of particulate protein size on hydrolysis in anaerobic digestion. Ind. Eng. Chem. Res. 50, 10843–10849. doi:10.1021/ie200385e

APHA, AWA, WEF, 2012. Standard method for examination of water and wastewater, 22nd ed. American Public Health Association, Washington.

Asano, T., Levine, A.D., 1998. Wastewater reclamation, recycling and reuse: An introduction,

in: Asano, T. (Ed.), Wastewater Reclamation and Reuse: Water Quality Management Library, Volume X. CRC Press, Boca Raton, pp. 1–56.

Bagi, A., Pampanin, D.M., Lanzén, A., Bilstad, T., Kommedal, R., 2014. Naphthalene biodegradation in temperate and arctic marine microcosms. Biodegradation 25, 111–125. doi:10.1007/s10532-013-9644-3

Cheong, K.-L., Wu, D.-T., Zhao, J., Li, S.-P., 2015. A rapid and accurate method for the quantitative estimation of natural polysaccharides and their fractions using high performance size exclusion chromatography coupled with multi-angle laser light scattering and refractive index detector. J. Chromatogr. A 1400, 98–106. doi:10.1016/j.chroma.2015.04.054

Cheryan, M., 1998. Ultrafiltration and microfiltration handbook. CRC Press, Boca Raton, Florida.

Choubert, J.M., Rieger, L., Shaw, A., Copp, J., Spérandio, M., Sørensen, K., Rönner-Holm, S., Morgenroth, E., Melcer, H., Gillot, S., 2013. Rethinking wastewater characterisation methods for activated sludge systems - A position paper. Water Sci. Technol. 67, 2363–2373. doi:10.2166/wst.2013.158

Dimock, R., Morgenroth, E., 2006. The influence of particle size on microbial hydrolysis of protein particles in activated sludge. Water Res. 40, 2064–2074. doi:10.1016/j.watres.2006.03.011

Doğruel, S., 2012. Biodegradation characteristics of high strength municipal wastewater supported by particle size distribution. Desalin. Water Treat. 45, 11–20. doi:10.1080/19443994.2012.691955

Dulekgurgen, E., Doğruel, S., Karahan, Ö., Orhon, D., 2006. Size distribution of wastewater COD fractions as an index for biodegradability. Water Res. 40, 273–282. doi:10.1016/j.watres.2005.10.032

494 Fox, P.F., McSweeney, P.L.H., 2006. Advanced Dairy Chemistry: Vol 2 Lipids., 3rd ed.
495 Springer, New York.
496 Gorini, D., Choubert, J.M., Le Pimpec, P., Heduit, A., 2011. Concentrations and fate of
497 sugars, proteins and lipids during domestic and agro-industrial aerobic treatment. Water
498 Sci. Technol. 63, 1669–1677. doi:10.2166/wst.2011.334
499 Harmsen, G.J., 2007. Reactive distillation : The front-runner of industrial process
500 intensification A full review of commercial applications, research, scale-up, design and
501 operation. Chem. Eng. Process. 46, 774–780. doi:10.1016/j.cep.2007.06.005
502 Henze, M., Harremoës, P., la Cour Jansen, J., Arvin, E., 2002. Wastewater treatment.
503 Springer, Berlin.
504 Huang, M., Li, Y., Gu, G., 2010. Chemical composition of organic matters in domestic
505 wastewater. Desalination 262, 36–42. doi:10.1016/j.desal.2010.05.037
506 Hvitved-Jacobsen, T., Vollertsen, J., Matos, J.S., 2002. The sewer as a bioreactor - a dry
507 weather approach. Water Sci. Technol. 45, 11–24.
508 Jones, L.J., Haugland, R.P., Singer, V.L., 2003. Development and characterization of the
509 NanoOrange protein quantitation assay: A fluorescence-based assay of proteins in
510 solution. Biotechniques 34, 850–861.
511 Karahan, Ö., Dogruel, S., Dulekgurgen, E., Orhon, D., 2008. COD fractionation of tannery
512 wastewaters-Particle size distribution, biodegradability and modeling. Water Res. 42,
513 1083–1092. doi:10.1016/j.watres.2007.10.001
514 Kommedal, R., Milferstedt, K., Bakke, R., Morgenroth, E., 2006. Effects of initial molecular
515 weight on removal rate of dextran in biofilms. Water Res. 40, 1795–1804.
516 doi:10.1016/j.watres.2006.02.032
517 Kommedal, R., Ydstebø, L., Bilstad, T., 2016. Occurrence and fate of priority organic
518 pollutants during wastewater sludge treatment, in: 5th International Conference on

519 Industrial and Hazardous Waste Management, 27-30th September 2016, Chania, Crete.
520 Levine, A.D., Tchobanoglous, G., Asano, T., 1991. Size distributions of particulate
521 contaminants in wastewater and their impact on treatability. Water Res. 25, 911–922.
522 doi:10.1016/0043-1354(91)90138-G
523 Leyva, A., Quintana, A., Sánchez, M., Rodríguez, E.N., Cremata, J., Sánchez, J.C., 2008.
524 Rapid and sensitive anthrone-sulfuric acid assay in microplate format to quantify
525 carbohydrate in biopharmaceutical products: Method development and validation.
526 Biologicals 36, 134–141. doi:10.1016/j.biologicals.2007.09.001
527 Logan, B.E., Jiang, Q., 1990. Molecular size distribution of dissolved organic matter. J.
528 Environ. Eng. 116, 1046–1062.
529 Matassa, S., Batstone, D.J., Hülsen, T., Schnoor, J., Verstraete, W., 2015. Can direct
530 conversion of used nitrogen to new feed and protein help feed the world? Environ. Sci.
531 Technol. 49, 5247–5254. doi:10.1021/es505432w
532 Puchongkawarin, C., Gomez-Mont, C., Stuckey, D.C., Chachuat, B., 2015. Chemosphere
533 Optimization-based methodology for the development of wastewater facilities for energy
534 and nutrient recovery. Chemosphere 140, 150–158.
535 doi:10.1016/j.chemosphere.2014.08.061
536 Puyol, D., Batstone, D.J., Hülsen, T., Astals, S., Peces, M., Krömer, J.O., 2017. Resource
537 recovery from wastewater by biological technologies: Opportunities, challenges, and
538 prospects. Front. Microbiol. 7, 1–23. doi:10.3389/fmicb.2016.02106
539 Raunkjær, K., Hvitved-Jacobsen, T., Nielsen, P.H., 1994. Measurement of pools of protein,
540 carbohydrate and lipid in domestic wastewater. Water Res. 28, 251–262.
541 Ravndal, K.T., Kommedal, R., 2017. Starch degradation and intermediate dynamics in
542 flocculated and dispersed microcosms. Water Sci. Technol. In Press.
543 doi:10.2166/wst.2017.467

Ravndal, K.T., Künzle, R., Derlon, N., Morgenroth, E., 2015. On-site treatment of used wash-water using biologically activated membrane bioreactors operated at different solids retention times. J. Water Sanit. Hyg. Dev. 4, washdev2015174. doi:10.2166/washdev.2015.174

Roeleveld, P.J., Van Loosdrecht, M.C.M., 2002. Experience with guidelines for wastewater characterisation in The Netherlands. Water Sci. Technol. 45, 77–87.

Ruiken, C.J., Breuer, G., Klaversma, E., Santiago, T., van Loosdrecht, M.C.M., 2013. Sieving wastewater - Cellulose recovery, economic and energy evaluation. Water Res. 47, 43–48. doi:10.1016/j.watres.2012.08.023

Ryckebosch, E., Muylaert, K., Foubert, I., 2012. Optimization of an analytical procedure for extraction of lipids from microalgae. JAOCS, J. Am. Oil Chem. Soc. 89, 189–198. doi:10.1007/s11746-011-1903-z

Sophonsiri, C., Morgenroth, E., 2004. Chemical composition associated with different particle size fractions in municipal, industrial, and agricultural wastewaters. Chemosphere 55, 691–703. doi:10.1016/j.chemosphere.2003.11.032

Sutton, P.M., Melcer, H., Schraa, O.J., Togna, A.P., 2011. Treating municipal wastewater with the goal of resource recovery. Water Sci. Technol. 63, 25–31. doi:10.2166/wst.2011.004

Tran, N.H. an, Ngo, H.H. ao, Urase, T., Gin, K.Y. ew H., 2015. A critical review on characterization strategies of organic matter for wastewater and water treatment processes. Bioresour. Technol. 193, 523–533. doi:10.1016/j.biortech.2015.06.091

van Loosdrecht, M.C.M., Brdjanovic, D., 2014. Anticipating the next century of wastewater treatment. Science. 344, 1452–1453. doi:10.1126/science.1255183

van Nieuwenhuijzen, A.F., van der Graaf, J.H.J.M., Kampschreur, M.J., Mels, A.R., 2004. Particle related fractionation and characterisation of municipal wastewater. Water Sci.

Technol. 50, 125–132.

Verstraete, W., Van de Caveye, P., Diamantis, V., 2009. Maximum use of resources present in domestic “used water.” Bioresour. Technol. 100, 5537–5545. doi:10.1016/j.biortech.2009.05.047

Wahlen, B.D., Willis, R.M., Seefeldt, L.C., 2011. Biodiesel production by simultaneous extraction and conversion of total lipids from microalgae, cyanobacteria, and wild mixed-cultures. Bioresour. Technol. 102, 2724–2730. doi:10.1016/j.biortech.2010.11.026

Wang, X., McCarty, P.L., Liu, J., Ren, N.-Q., Lee, D.-J., Yu, H.-Q., Qian, Y., Qu, J., 2015. Probabilistic evaluation of integrating resource recovery into wastewater treatment to improve environmental sustainability. Proc. Natl. Acad. Sci. 112, 1630–1635. doi:10.1073/pnas.1410715112

Wilsenach, J.A., Maurer, M., Larsen, T.A., van Loosdrecht, M.C., 2003. From waste treatment to integrated resource management. Water Sci. Technol. 48, 1–9.

Wyatt, P.J., 1993. Light scattering and the absolute characterization of macromolecules. Anal. Chim. Acta 272, 1–40.

Wyatt Technology (2017) https://www.wyatt.com/solutions/techniques/sec-mals-molar-mass-size-multi-angle-light-scattering.html accessed on 12 December, 2017.

Zhao, H., Brown, P.H., Schuck, P., 2011. On the distribution of protein refractive index increments. Biophys. J. 100, 2309–2317. doi:10.1016/j.bpj.2011.03.004

Zhu, F., Wu, X., Zhao, L., Liu, X., Qi, J., Wang, X., Wang, J., 2017. Lipid profiling in sewage sludge 116. doi:10.1016/j.watres.2017.03.032

Zhu L. Nugroho Y.K., Shakeel S.R., Li Z., Martinkauppi B. and Hiltunen E. (2017) Using microalgae to produce liquid transportation biodiesel: What is next? Renewable and Sustainable Energy Reviews, 78, 391-400. doi: 10.1016/j.rser.2017.04.089

Table 1: Concentration of COD, total-N, total-P, carbohydrate, proteinaceous material, total oils and fats, and total lipids and free fatty acids in raw wastewater (WW), TSS filtrate and all size fractions from Vik wastewater (± standard error)

Fraction	COD (mg L^{-1})	Total-N (mg N L^{-1})	Total-P (mg P L^{-1})	Carbohydrate (mg COD L^{-1})	Proteinaceous material (mg COD L^{-1})	Oils and fats (mg COD L^{-1})	Lipids and free fatty acids (mg COD L^{-1})	Unidentified (mg COD L^{-1})	Inert (mg COD L^{-1})	Biodegradable (mg COD L^{-1})
Raw WW	1421 ± 58	62 ± 6	10.7 ± 0.6	165 ±.8	12.6 ± 0.6	382 ± 16	310 ± 1	862 ± 61	506 ± 21	915 ± 38
TSS filtrate	590 ± 7	43 ± 1	6.62 ± 0.04	n/a	n/a	n/a	n/a	n/a	n/a	n/a
> 1 mm	113 ± 4	1.13 ± 0.05	0.30 ± 0.07	109 ± 45	0.72 ± 0.04	18.4 ± 0.6	14.74 ± 0.04	0	17 ± 1	97 ± 7
100 µm – 1 mm	51 ± 4	0.82 ± 0.05	0.19 ± 0.01	39 ± 18	1.4 ± 0.5	8.9 ± 0.4	5.69 ± 0.06	1 ± 18	15 ± 2	36 ± 4
25 – 100 µm	32.2 ± 0.6	0.76 ± 0.02	0.144 ± 0.003	5.9 ± 0.4	0.9 ± 0.2	15.1 ± 0.5	10.3 ± 0.5	10 ± 1	7.6 ± 0.5	25 ± 2
0.65 – 25 µm	318 ± 2	5.4 ± 0.4	1.03 ± 0.05	16 ± 2	9.7 ± 0.4	225 ± 3	200 ± 1	67 ± 5	54 ± 4	263 ± 17
0.1 – 0.65 µm	3.14 ± 0.08	0.150 ± 0.002	0.025 ± 0.002	0.41 ± 0.05	< 0.04	n/a	n/a	2.7 ± 0.1	1.66 ± 0.06	1.49 ± 0.05
1000 kDa – 0.1 µm	0.38 ± 0.04	0.016 ± 0.002	0.0039 ± 0.0004	< 0.15	< 0.04	1.4 ± 0.1	1.2 ± 0.9	0	0.20 ± 0.02	0.18 ± 0.02
100 – 1000 kDa	0.83 ± 0.02	0.050 ± 0.002	0.0082 ± 0.0003	0.23 ± 0.03	< 0.04	1.6 ± 0.1	1 ± 1	0	0.29 ± 0.03	0.54 ± 0.06
10 – 100 kDa	4.30 ± 0.02	0.317 ± 0.02	0.040 ± 0.002	0.9 ± 0.1	0.26 ± 0.02	3.6 ± 0.2	1 ± 1	0	0.54 ± 0.04	3.8 ± 0.3
1 – 10 kDa	16.4 ± 0.1	1.07 ± 0.02	0.093 ± 0.002	5.2 ± 0.6	0.63 ± 0.08	6.2 ± 0.2	0.152 ± 0.002	4.4 ± 0.7	0.5 ± 0.3	16 ± 12
< 1 kDa	567 ± 5	36.3 ± 1	6.5 ± 0.2	66 ± 8	1.72 ± 0.08	149 ± 9	0.00 ± 0.00	351 ± 13	161 ± 5	406 ± 13
Recovery (%)	78 ± 3	74 ± 8	78 ± 5	147 ± 30	122 ± 8	112 ± 5	75.7 ± 0.8	50 ± 4	51 ± 2	93 ± 5

Table 2: Concentration of COD, total-N, total-P, carbohydrate, proteinaceous material, total oils and fats, and total lipids and free fatty acids in raw wastewater (WW), TSS filtrate and all size fractions from Mekjarvik wastewater (± standard error)

Fraction	COD (mg L^{-1})	Total-N (mg N L^{-1})	Total-P (mg P L^{-1})	Carbohydrate (mg COD L^{-1})	Proteinaceous material (mg COD L^{-1})	Oils and fats (mg COD L^{-1})	Lipids and free fatty acids (mg COD L^{-1})	Unidentified (mg COD L^{-1})	Inert (mg COD L^{-1})	Biodegradable (mg COD L^{-1})
Raw WW	690 ± 30	37 ± 1	5.0 ± 0.2	395 ± 16	39.9 ± 0.8	209 ± 12	106 ± 2	47 ± 36	191 ± 10	499 ± 27
TSS filtrate	262 ± 10	27 ± 1	2.6 ± 0.2	n/a	n/a	n/a	n/a	n/a	121 ± 6	142 ± 7
> 1 mm	139 ± 5	0.53 ± 0.02	0.286 ± 0.003	149 ± 23	1.09 ± 0.02	37.3 ± 0.6	21.4 ± 0.1	0	11 ± 3	128 ± 37
100 µm – 1 mm	27 ± 4	0.37 ± 0.02	0.053 ± 0.002	45 ± 5	0.31 ± 0.04	5.5 ± 0.2	4.5 ± 0.5	0	5.6 ± 0.8	22 ± 3
25 – 100 µm	37.2 ± 0.8	1.07 ± 0.03	0.184 ± 0.004	11.1 ± 0.3	1.04 ± 0.05	17.9 ± 0.5	11.7 ± 0.1	7 ± 1	5.3 ± 0.5	32 ± 3
0.65 – 25 µm	101.6 ± 0.9	3.4 ± 0.2	0.71 ± 0.03	15.4 ± 0.3	1.9 ± 0.1	45.4 ± 0.4	30.9 ± 0.4	39 ± 1	2.5 ± 0.5	99 ± 18
0.1 – 0.65 µm	0.64 ± 0.02	0.0412 ± 0.0005	0.0053 ± 0.0007	0.47 ± 0.01	0.022 ± 0.002	0.00 ± 0.00	0.044 ± 0.001	0.13 ± 0.03	0.06 ± 0.04	0.6 ± 0.4
1000 kDa – 0.1 µm	0.20 ± 0.02	0.0264 ± 0.0005	0.0035 ± 0.0007	0.54 ± 0.03	0.023 ± 0.002	0.00 ± 0.00	0.08 ± 0.04	0	0.035 ± 0.003	0.17 ± 0.02
100 – 1000 kDa	0.382 ± 0.009	0.0345 ± 0.0004	0.0036 ± 0.0006	0.52 ± 0.03	0.026 ± 0.002	0.00 ± 0.00	0.04 ± 0.07	0	0	0.382 ± 0.009
10 – 100 kDa	2.6 ± 0.3	0.0065 ± 0.0006	0.0071 ± 0.0009	1.36 ± 0.05	0.080 ± 0.003	0.00 ± 0.00	0.021 ± 0.002	1.2 ± 0.3	0.71 ± 0.09	1.9 ± 0.3
1 – 10 kDa	6.36 ± 0.06	0.244 ± 0.009	0.024 ± 0.001	1.7 ± 0.2	0.42 ± 0.01	6.4 ± 0.2	0.299 ± 0.001	0	1.2 ± 0.2	5.2 ± 0.8
< 1 kDa	363 ± 5	25 ± 1	2.9 ± 0.2	108 ± 2	5.9 ± 0.4	25 ± 3	7.68 ± 0.09	224 ± 6	233 ± 6	131 ± 3
Recovery (%)	98 ± 4	83 ± 4	83 ± 4	84 ± 7	27 ± 1	66 ± 4	72 ± 2	580 ± 448	136 ± 8	84 ± 9

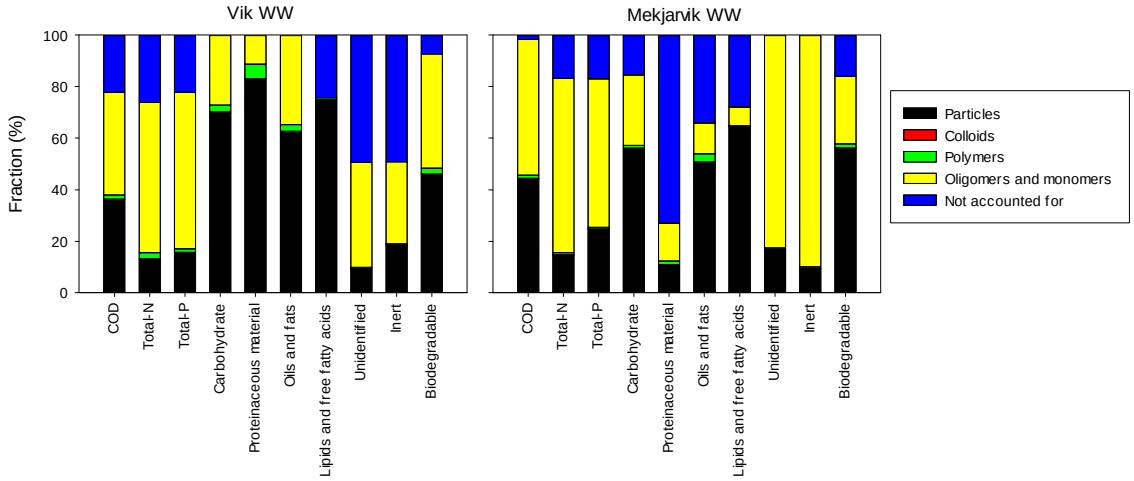

Figure 1: Size distribution of OM in particulate (>0.65 µm), colloidal (1000 kDa – 0.65 µm), polymeric (1-1000 kDa) and truly dissolved (< 1 kDa) size ranges. Calculations are based on raw wastewater measurement except for carbohydrate, proteinaceous material, and oils and fats for Vik wastewater, and unidentified and inert material for Mekjarvik wastewater, where the sum of material in the size fractions is used due to a recovery higher than 100 %

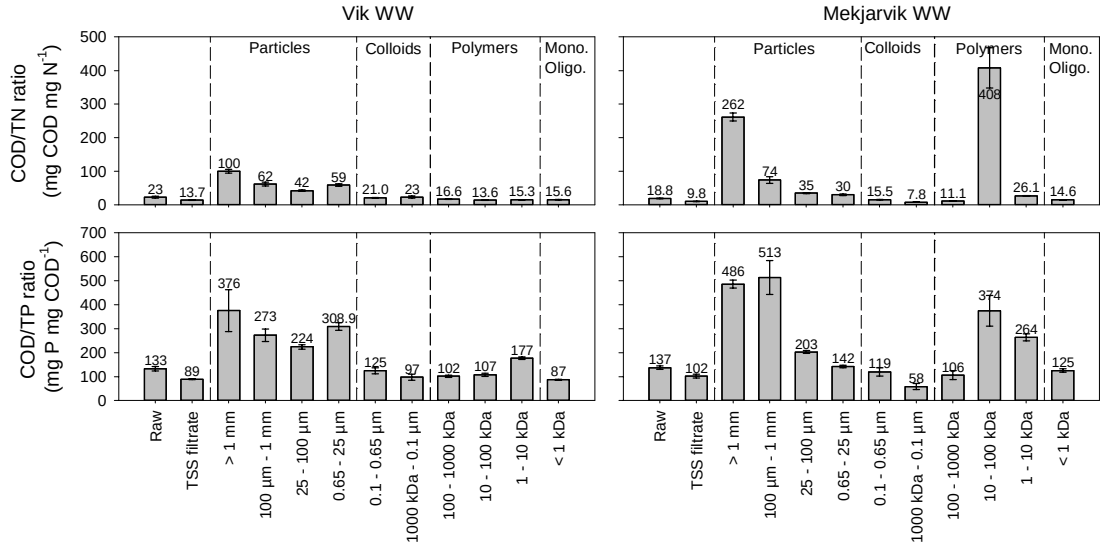

Figure 2: COD/TN and COD/TP in raw wastewater and all size fractions for Vik and Mekjarvik wastewater. Error bars show standard deviations calculated for relative values.

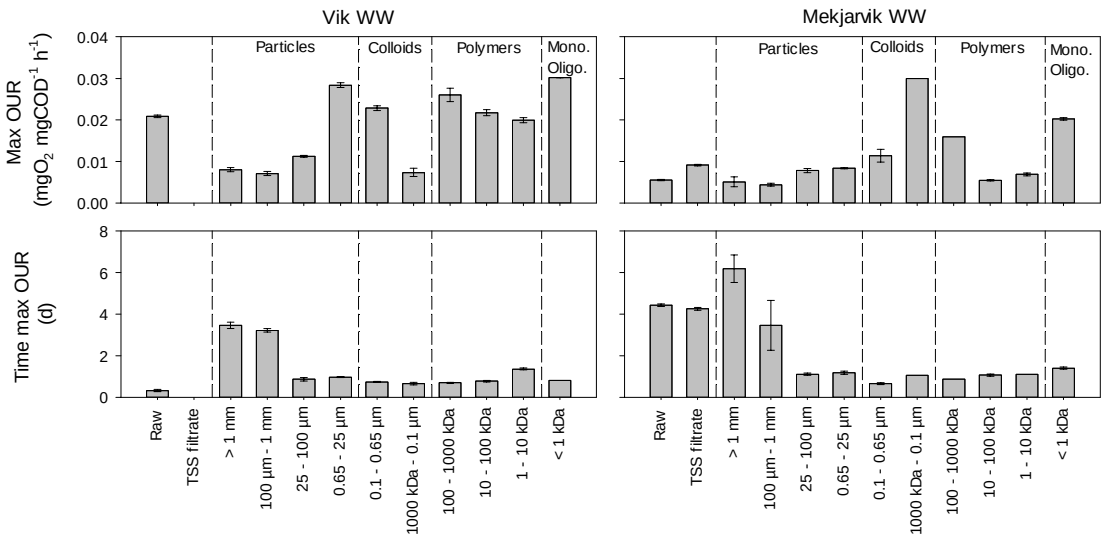

Figure 3: Max OUR (mg O_2 mg COD^{-1} h^{-1}) and time to reach max OUR (d). Error bars show standard error. *) 1000 kDa – 0.1 µm and 100-1000 kDa fraction Mekjarvik wastewater data from only one parallel, the rest average of data from three parallels.

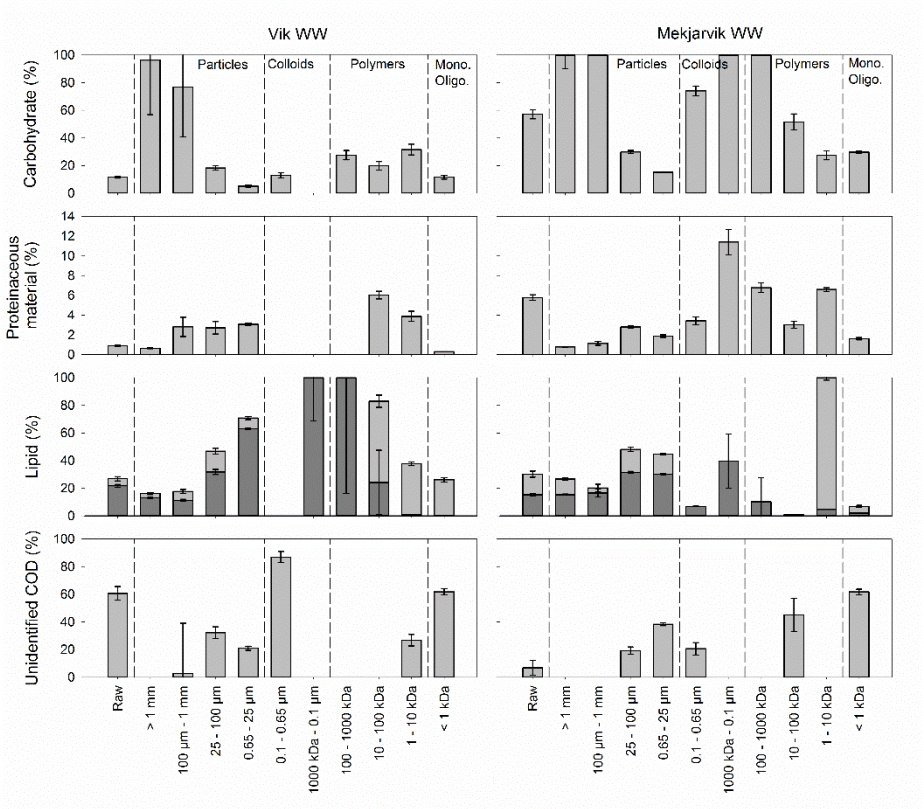

Figure 4: Content of carbohydrate, proteinaceous material, lipids as total oils and fats (light grey) and total lipids and fatty acids (dark grey), and unidentified COD in raw wastewater and all size fractions for Vik and Mekjarvik wastewater. Percentage was calculated as percentage of measured COD in each individual fraction. Error bars show standard deviations calculated for relative values.

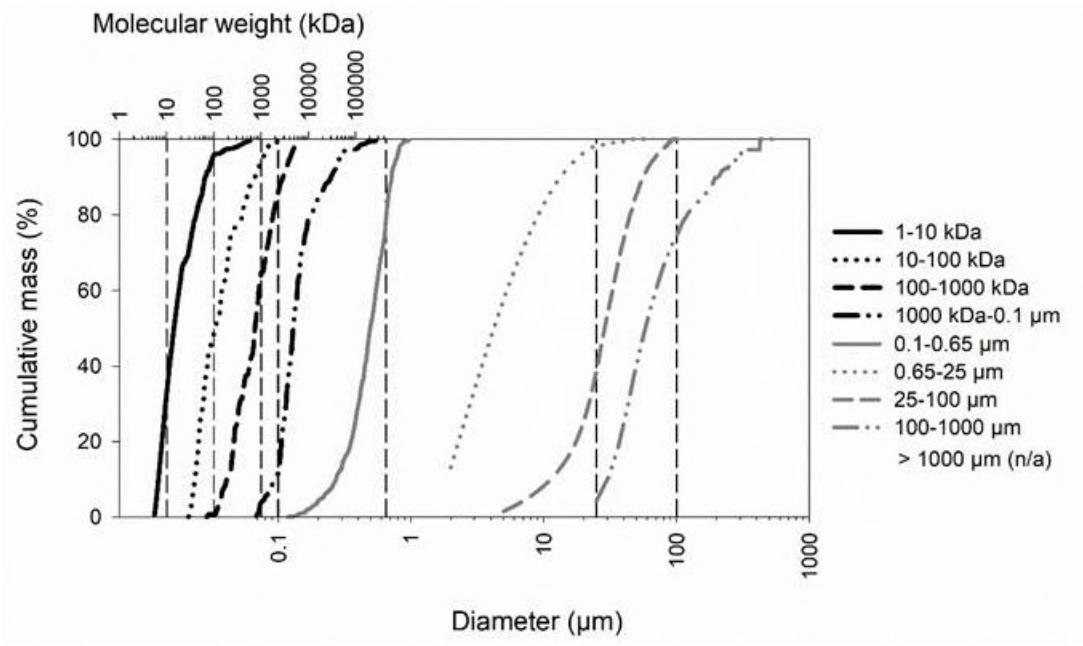

Figure 5: Analysed size distribution in size fractionated wastewater from Mekjarvik WWTP. Particulate fractions are based on volume measurements and density was assumed constant between fractions.

Supplementary information

A. Serial filtration of wastewater

Figure A1 shows the WW-fractionation setup, the left section shows the initial sieving while the right section shows the tangential flow filtration (TFF) stages. During the sieving process, raw wastewater was fed with a peristaltic pump onto a column holding the three sieves with consecutively smaller cut-offs. A small amount of washing water (Milli-Q pH 2.3 adjusted with HCl) was used to remove trapped sub-fraction particles. The amount of washing water was recorded and the water itself was pooled together with the rest of filtered WW. The sieving-filtrate was then transferred to the TFF feed tank (first pass). During the TFF, the system was run in a continuously fed batch mode until all the water had passed through each filter. The first TFF run was carried out with the 0.65 µm cutoff filter. At the end of the run, a small amount of washing water was added to the concentrate to wash out salts and trapped sub-fraction particles. Again, the amount of the washing water was measured and the water itself was pooled together with the filtrate. This washing step was carried out at each filtration stage. The fraction concentrate was drained from the lowest point of the TFF system unassisted until it stopped flowing. Finally, the filtrate was returned to the clean and emptied TFF feed tank and the process was repeated using the next filter (0.1 µm cutoff). Similarly, four more rounds were carried out with to complete the size fractionation. Throughout the entire TFF process, temperatures were logged externally for the concentrate tank, feed tank, membrane filter and filtrate tanks. Feed, transmembrane and delta pressures were also logged in order to keep track of filter performance. The weight of concentrate was set as a trigger to stop the process preventing running the system dry. In addition, coolant loops and heat

exchangers where either submerged in tanks or placed in line to keep the wastewater cool. The WW were also continuously mixed at 200 rpm or circulated to prevent settling.

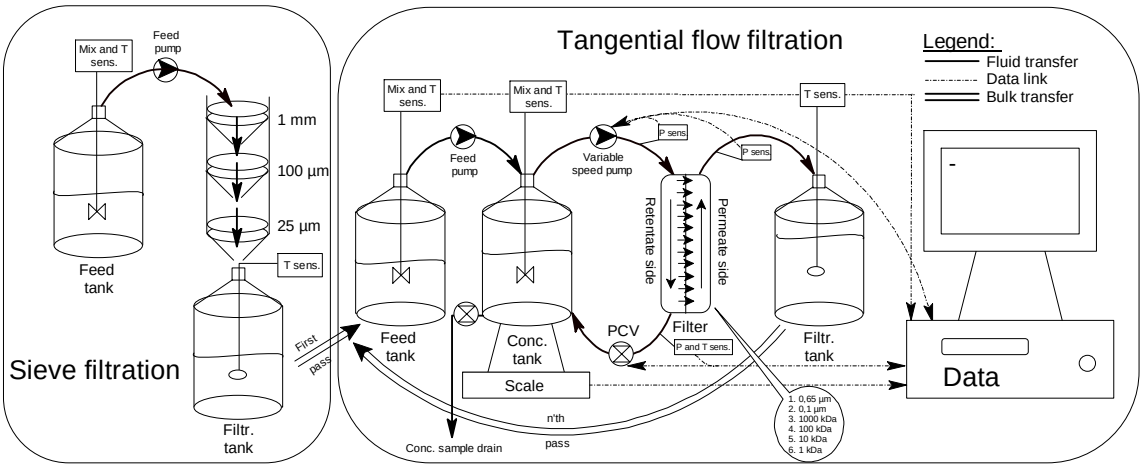

Figure A1: Experimental setup of the serial filtration process. The wastewater was first sieved, followed by micro and ultrafiltration with a tangential flow filtration setup.

B. Determination of lipids content in wastewater

Total oils and fats extraction

All glassware and volumetric equipment were rinsed using a 1:1 mixture of analytical grade Methanol (NOMAPURE, VWR Int.) and Chloroform (EMSURE, Merck GmbH). Volumetric aliquots (about 10 ml) of concentrated fractionated wastewater was quantitatively transferred to Teflon sealed 200 ml Schott bottles (Duran Group GmBH) and mixed with 20 ml Chloroform and 20 ml Methanol. Lipids were extracted for a minimum of 2 hours on a shaker, intermittently sonicated for 2x8 min on a Branson 2510 sonicator at 50°C/100 W (Branson Ultrasonics, Danbury CT, USA). Following extraction, the mixture was quantitatively transferred to a 250 ml separation funnel and left overnight for phase separation. The lower fraction was collected, and the liquid re-extracted two times by shaking using 20 ml Chloroform and 10 ml deionized water. The

combined extract was transferred to a Syncore analyst (BÜCHI Labortechnik AG, CH), vacuum distiller and concentrated to < 1 ml (at 55°C and 250 mbar A). The concentrate was quantitatively transferred to a Teflon lined 10 ml vial using an additional 3-4 ml Chloroform and stored in the dark at 4°C.

Clean up

Extracted samples were transferred to 15 ml conical Duran glass centrifuge tubes and added 1 ml distilled water, vortexed and centrifuged at 1000 g for 5 min. The upper layer was removed using a Pasteur pipette, while the lower Chloroform layer was transferred to an anhydrous Na_2SO_4 packed glass column for residual water removal. The removed water layer was transferred back to the centrifuge tube, and re-extracted using 5 ml of 1:1 Chloroform-Methanol and dried over the same column (same procedure as above). The combined extracts were evaporated to dryness by a gentle stream of Argon inside a 50°C heat block, and resuspended in 2 ml Toluene:Methanol (2:1). 1 ml was transferred to a 2 ml glass vial for gravimetric determination of total oil and fats, while the remaining sample (1.00 ml) was used for total lipids determination.

Gravimetric determination of total oils and fats

The 1.00 ml oil and fats extract was evaporated to dryness in a Visiprep SPE Vacuum manifold (Supelco Inc) to dryness by a gentle stream of Argon at 250 mbar A. Following vacuum drying, the sample was weighed using a high precision analytical balance (0.01 mg resolution, Mettler Toledo model XSE). The vial was dried for another 15 min until constant weight. Total oils and fats was removed using repeated flushing using a 1:1 Chloroform – Methanol mixture, and the vials were vacuum dried until constant weight.

Total oils and fats was determined as the differential weight before and after oil and fats removal.

Derivatisation and analysis of total lipids

Total lipids and fatty acids composition was determined by GC-FID following transesterification and methylation of lipids into fatty acid methyl esters (FAME) according to Ryckebosch et al. (2012). 1 ml of fresh 2% (v/v) sulfuric acid (pro analysis, VWR Int.) in methanol (NOMAPURE, VWR Int.) was added to the remaining 1.00 ml total oils and fats extract (above). The sample was vortexed and left for lipids methylation for 1 hour at 80°C. After methylation and cooling to room temperature, 0.5 ml 5 M aqueous NaCl solution was added and sample vortexed, followed by addition of 2 ml Hexane (HiPerSolv CHROMANORM® for HPLC, VWR chemicals) and vortexing. The samples were centrifuged for 2 min at 1000 g, and the upper layer transferred to a glass column packed with anhydrous Na_2SO_4 for drying. Samples were re-extracted by another 2 ml Hexane and 1 ml water, centrifuged and the hexane layer dried and combined with the initial upper layer. The methylated extract was dried under a gentle stream of Argon at 50°C (in heat block), and upon drying, resuspended in 1000 µl Hexane:Chloroform (2:1) mixture for GC analysis.

FAME distribution and quantification was determined using an Agilent 6890 gas chromatograph equipped with an Agilent J&W DB-225MS capillary column (PN 122-2932) operated in constant pressure mode, using Helium as carrier gas. 1 µl sample was injected using a Gerstel MPS liquid mode sampler onto a 220°C pulsed split inlet (50:1 split ratio, at 350 kPa for initial 0.5 min, followed by 93 kPa run pressure). The initial oven temperature was 50°C, followed by an immediate ramp of 26°C/min to 200°C, and a final ramping to 230°C at 2.7°C/min (hold for 11.12 min) to give a total runtime of 28

min. FAME's where detected by a flame ionization detector kept at 240°C operated in constant makeup mode. Quantification and retention time identification was achieved by external standard calibration using a five point dilution series of certified Supelco 37 component FAME mix standard (Supelco, Sigma-Aldrich) containing 37 FAME standards from C4:0 to C24:6 methylated fatty acids. Retention time confirmation and unknown peak identification were perfomed under the same capillary column and GC conditions, but using a quadropole mass selective detector (Agilent 5975) operated in SCAN EI mode (scan range 35 to 400 amu at 70 eV) and a source and quad temperature of 180 and 150°C, respectively. Unknown peaks and standard peak eluation order verification were done by identification using NIST library comparison (Agilent NIST bundle version 05).

Recovery and quality control

Matrix recovery was determined by addition of a known amount of commercial olive oil (31.86 mg) to three replicates of SNJ 25-100 µm fraction sample. Results showed a stable sample matrix recovery of 70 ± 2 % for FAME determination, and 86±1 % for gravimetric determination of oil and fats. All sample analytical results were compensated using these recovery factors. A quality standard of 2 mg lipids sample using commercial olive oil, was prepared and used for analytical stability and recovery checks. External calibration standards were co-analyzed with samples to correct for retention time drifting and FID response factor compensation.

C. Solids and nutrient content in wastewater

Concentrations of total COD, TSS, VSS, ammonia, nitrate and phosphate in Vik and Mekjarvik WW are provided in table C1.

Table C1: Concentrations of total COD, TSS, VSS, ammonia, nitrate and phosphate in Vik and Mekjarvik WW (± standard error)

	Vik WW	**Mekjarvik WW**
COD	1421 ± 58	690 ± 30
TSS (mg L^{-1})	371 ± 4	262 ± 13
VSS (mg L^{-1})	343 ± 4	222 ± 10
NH_4^+ (mg N L^{-1})	30.3 ± 0.3	22.7 ± 0.5
NO_3^- (mg N L^{-1})	< 0.5	< 0.5
PO_4^{3-} (mg P L^{-1})	5.70 ± 0.06	2.53 ± 0.03

D. Correlations of total-N, total-P and chemical components

Nitrogen and phosphorous content of COD was compared with carbohydrate, proteinaceous material, total oils and fats, total lipids and free fatty acids, and unidentified COD by testing for correlations based on Pearson product-moment correlation coefficients (table D1). For this analysis, ammonia and phosphate concentrations was substracted from total-N and total-P data for raw WW and for the < 1 kDa fraction.

Table D1: Correlation between proteinaceous material, carbohydrate, total oils and fats, total lipids and free fatty acids and unidentified COD content (%) with total-N (TN/COD) and total-P (TP/COD) content. Correlations based on Pearson product-moment correlation coefficients, correlations are considered significant if P-values < 0.05

	Vik WW			**Mekjarvik WW**		
	Correlation Coefficient	**P-value**	**Significant**	**Correlation Coefficient**	**P-value**	**Significant**
Carbohydrate vs total-N	-0.28	0.4	No	0.66	0.03	Yes
Proteinaceous material vs total-N	0.84	0.009	Yes	0.84	0.001	Yes
Total oils and fats vs total-N	0.38	0.3	No	-0.16	0.6	No
Total lipids and free fatty acids vs total-N	0.24	0.5	No	0.46	0.2	No
Unidentified vs total-N	-0.18	0.6	No	-0.42	0.2	No
Carbohydrate vs total-P	-0.22	0.5	No	0.64	0.03	Yes
Proteinaceous material vs total-P	0.92	0.001	Yes	0.79	0.004	Yes
Total oils and fats vs total-P	0.78	0.008	Yes	-0.20	0.6	No
Total lipids and free fatty acids vs total-P	0.69	0.03	Yes	0.60	0.05	Yes
Unidentified vs total-P	-0.30	0.4	No	-0.33	0.3	No

E. First order simulation of BOD

For Vik WW, biological oxygen demand (BOD) was measured over 7 days for raw WW and 14 days for all size fractions (figure E1). For Mekjarvik WW, BOD was measured over 21 days for all samples (figure E1). Modelling BOD curves using first order kinetics generally has its limitations due to the models inability to follow complex degradation patterns. Especially for large particulate fractions with slower initial degradation and a distinct bimodal growth phase, the first order model gave a bad fit (figure E1). Bimodal growth was a result of initial fast growth of readily degradable particles, followed by degradation of slowly degradable particles. Bimodal growth was also observed in the smaller size fractions, however these had a faster initial growth, followed by a slower second growth period. However, for most fractions the first order model will reach a representable ultimate BOD level, thus a representable inert fraction was estimated.

The second growth phase observed in several fractions after 12 days for Vik WW and 15 days for Mekjarvik WW (figure E1) were most likely due to nitrification. No nitrification inhibitor was used during BOD tests due to possible degradation of the inhibitor itself, which would lead to interference with the BOD measurements. This is normally checked using parallel controls, but limited instrumental capacity did not allow for this in this experiment. The smaller size fractions have a late second growth phase, and in general has a lower COD/TN ratio than the particulate fractions (figure 2). On the contrary, the 10-100 kDa fraction of Mekjarvik WW had a very high COD/TN ratio and does not have a second growth phase further supporting this to be an effect of nitrification.

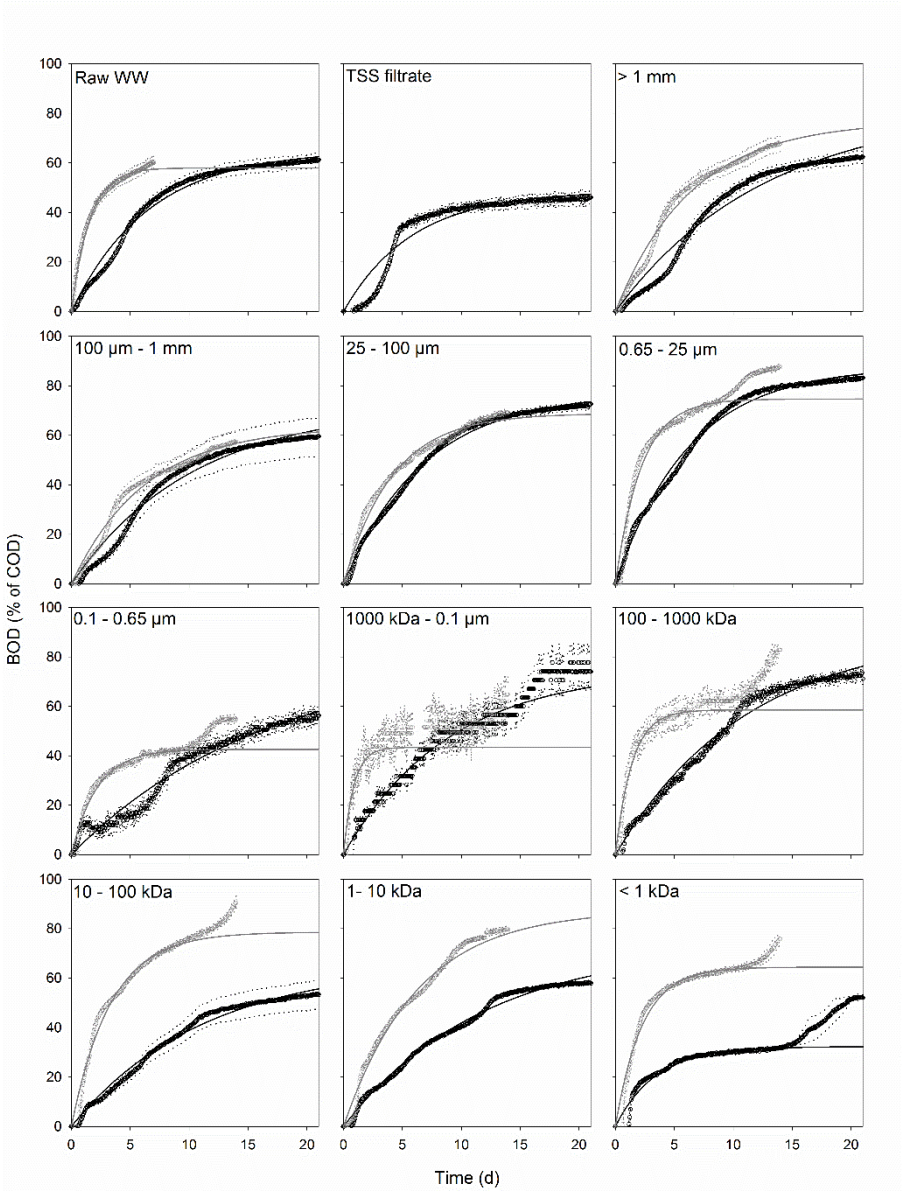

Figure E1: BOD as % of initial COD value for Vik WW (grey) and Mekjarvik WW (black). Dotted lines show standard deviations calculated for relative values, and solid lines show 1.order simulation of BOD data modelled after Roeleveld and van Loosdrecht (2002). *) 1000 kDa – 0.1 µm and 100-1000 kDa fraction data from Mekjarvik WW from one parallel only.

Inert COD fractions was estimated based on the method proposed by Roeleveld and van Loosdrecht (2002). First order kinetics was used to estimate ultimate biodegradable COD (BCOD). Inert COD was then calculated by subtracting BCOD from initial COD.

Estimated first order rate constants (k_1) and estimated fraction of inert COD (f_{inert}) are presented in table E1.

Table E1: Estimated first order rate constants (k_1) and estimated fraction of inert COD in Vik and Mekjarvik WW. Estimations based on method proposed by Roeleveld and van Loosdrecht (2002).

Fraction	Vik WW		Mekjarvik WW	
	k_1 (h^{-1} mg COD^{-1})	f_{inert} (mg COD mg COD^{-1})	k_1 (h^{-1} mg COD^{-1})	f_{inert} (mg COD mg COD^{-1})
Raw WW	0.0033 ± 0.008	0.356 ± 0.002	0.00148 ± 0.00007	0.277 ± 0.009
TSS filtrate	n.a.	n.a.	0.0034 ± 0.0002	0.46 ± 0.01
> 1 mm	0.00078 ± 0.00005	0.146 ± 0.009	0.00075 ± 0.00006	0.08 ± 0.02
100 µm – 1 mm	0.00080 ± 0.00006	0.29 ± 0.02	0.0010 ± 0.0001	0.204 ±0.008
25 – 100 µm	0.00155 ± 0.00006	0.24 ± 0.01	0.00146 ± 0.00002	0.14 ± 0.01
0.65 – 25 µm	0.00238 ± 0.00006	0.17 ± 0.01	0.00159 ± 0.00001	0.025 ± 0.004
0.1 – 0.65 µm	0.00304 ± 0.00007	0.53 ± 0.01	0.0028 ± 0.0003	0.10 ± 0.06
1000 kDa – 0.1 µm	0.065 ± 0.006	0.52 ± 0.03	0.0026*	0.17*
100 – 1000 kDa	0.0172 ± 0.0007	0.35 ± 0.04	0.0011*	0.00*
10 – 100 kDa	0.00154 ± 0.00004	0.127 ± 0.009	0.0009 ± 0.0001	0.27 ± 0.02
1 – 10 kDa	0.00080 ± 0.00001	0.03 ± 0.02	0.00084 ± 0.00004	0.18 ± 0.03
< 1 kDa	0.00229 ± 0.00004	0.284 ± 0.009	0.0029 ± 0.0002	0.64 ± 0.01

*) data from one parallel

F. Lipids concentrations

Relative concentrations of lipids in Vik wastewater (table F1) and Mekjarvik wastewater (table F2) are calculated as percentage of total lipid concentration in the size fraction.

Table F1: Relative concentration of lipids in Vik wastewater (%)

	Raw	> 1 mm	100 µm – 1 mm	25 – 100 µm	0.65 – 25 µm	0.1 – 0.65 µm	1000 kDa – 0.1 µm	100 – 1000 kDa	10 – 100 kDa	1 – 10 kDa	< 1 kDa
C6:0	0.00	0.00	0.00	0.00	0.96		0.00	0.00	0.00	0.00	0.00
C8:0	0.00	0.00	0.00	0.00	0.89		0.00	0.00	0.00	0.00	0.00
C9:0	0.00	0.00	0.00	0.00	0.10		0.00	0.00	0.00	0.00	0.00
C10:0	0.00	0.00	0.00	0.00	2.25		0.00	0.00	0.00	0.00	0.00
C11:0	0.00	0.14	0.00	0.00	0.05		0.00	0.00	0.00	0.00	0.00
C12:0	0.42	1.92	0.00	0.85	4.21		0.00	0.00	0.00	0.00	0.00
C13:0	0.00	0.00	0.00	0.00	0.10		0.00	0.00	0.00	0.00	0.00
C14:0	6.93	5.78	3.43	6.55	12.37		0.00	0.00	0.00	0.00	0.00
C14:1	0.82	1.38	0.82	0.96	0.99		0.00	0.00	0.00	0.00	0.00
C15:0	1.02	0.61	0.70	0.88	0.06		0.00	0.00	0.00	0.00	0.00
C15:1	0.00	0.24	0.00	0.26	0.28		0.00	0.00	0.00	0.00	0.00
C16:0	39.52	29.75	27.99	31.91	36.91		11.73	5.63	10.42	30.63	0.00
C16:1	2.34	2.84	4.17	4.28	1.91		0.00	0.00	2.39	37.10	0.00
C17:0	0.52	0.55	0.92	1.32	0.70		8.46	0.00	0.00	0.00	0.00
C17:1	0.00	0.00	0.00	0.00	0.31		0.00	0.00	0.00	0.00	0.00
C18:0	17.19	19.44	16.35	17.30	13.04		25.06	15.72	17.91	9.62	0.00
C18:1n9	30.21	24.15	32.40	28.06	23.10		3.38	1.46	0.37	0.00	0.00
C18:2n6	0.47	6.83	8.59	2.84	0.08		0.00	0.00	0.00	0.00	0.00
C18:3n6	0.00	0.22	0.00	0.50	0.03		0.00	0.00	0.00	0.00	0.00
C18:3n3	0.55	2.98	1.67	0.57	0.17		0.00	0.00	0.00	0.00	0.00
C20:0	0.00	0.56	0.95	0.71	0.29		5.92	38.19	35.90	22.65	0.00
C20:1	0.00	0.23	0.00	0.17	0.20		2.68	35.61	33.00	0.00	0.00
C20:2	0.00	0.00	0.00	0.00	0.03		0.00	0.00	0.00	0.00	0.00
C20:3n6	0.00	0.00	0.00	0.00	0.08		0.00	0.00	0.00	0.00	0.00
C20:4n6	0.00	0.00	0.00	0.00	0.04		0.00	0.00	0.00	0.00	0.00
C21:0	0.00	0.00	0.00	0.00	0.04		0.00	0.00	0.00	0.00	0.00
C20:3n3	0.00	0.00	0.00	0.00	0.07		0.00	0.00	0.00	0.00	0.00
C20:5n3	0.00	0.00	0.00	0.84	0.06		0.00	0.00	0.00	0.00	0.00
C22:0	0.00	0.49	0.00	0.59	0.16		0.00	0.00	0.00	0.00	0.00
C22:1n9	0.00	0.00	0.00	0.00	0.02		0.00	0.00	0.00	0.00	0.00
C22:2	0.00	0.00	0.00	0.00	0.00		0.00	0.00	0.00	0.00	0.00
C23:0	0.00	1.90	2.01	1.41	0.38		0.00	3.39	0.00	0.00	0.00
C22:6n3	0.00	0.00	0.00	0.00	0.00		42.77	0.00	0.00	0.00	0.00
C24:0	0.00	0.00	0.00	0.00	0.11		0.00	0.00	0.00	0.00	0.00
C24:1	0.00	0.00	0.00	0.00	0.00		0.00	0.00	0.00	0.00	0.00

Table F2: Relative concentration of lipids in Mekjarvik wastewater (%)

	Raw	> 1 mm	100 µm – 1 mm	25 – 100 µm	0.65 – 25 µm	0.1 – 0.65 µm	1000 kDa – 0.1 µm	100 – 1000 kDa	10 – 100 kDa	1 – 10 kDa	< 1 kDa
C6:0	0.00	0.00	0.00	0.00	0.11	0.00	0.00	0.00	0.00	0.00	0.00
C8:0	0.00	0.00	0.00	0.00	0.20	0.00	0.00	0.00	0.00	0.00	0.00
C9:0	0.00	0.25	0.00	0.00	0.18	0.00	0.00	0.00	0.00	0.00	0.00
C10:0	0.00	0.08	0.00	0.00	0.66	0.00	0.00	0.00	0.00	0.00	0.00
C11:0	0.00	0.00	0.00	0.00	0.00	0.00	0.00	0.00	0.00	0.00	0.00
C12:0	0.00	1.30	0.00	1.09	2.36	0.00	0.00	0.00	0.00	4.93	0.00
C13:0	0.00	0.00	0.00	0.00	0.04	0.00	0.00	0.00	0.00	0.00	0.00
C14:0	19.64	3.17	2.14	3.43	6.48	0.00	0.00	0.00	0.00	0.00	0.00
C14:1	0.00	1.91	0.68	1.09	0.83	0.00	0.00	0.00	0.00	8.40	0.00
C15:0	0.00	0.54	0.45	0.70	1.00	0.00	0.00	0.00	0.00	0.00	0.00
C15:1	0.00	0.20	0.00	0.24	0.27	0.00	0.00	0.00	0.00	0.00	0.00
C16:0	21.30	25.55	21.40	25.74	30.39	35.89	4.84	0.00	17.46	14.54	0.00
C16:1	2.49	2.97	1.97	3.40	3.00	0.00	17.49	0.00	0.00	0.00	0.00
C17:0	0.00	0.67	0.34	1.03	0.93	0.00	0.00	0.00	0.00	0.00	100.00
C17:1	0.00	0.18	0.00	0.00	0.27	0.00	0.00	0.00	0.00	0.00	0.00
C18:0	19.99	15.66	16.87	20.22	22.29	64.11	13.90	0.00	49.95	0.00	0.00
C18:1n9	28.72	40.41	32.82	27.64	26.90	0.00	3.28	0.00	32.58	0.00	0.00
C18:2n6	7.88	0.15	9.99	8.80	0.24	0.00	0.00	0.00	0.00	0.00	0.00
C18:3n6	0.00	0.07	0.00	0.28	0.11	0.00	0.00	0.00	0.00	0.00	0.00
C18:3n3	0.00	0.16	1.10	1.09	0.22	0.00	0.00	0.00	0.00	0.00	0.00
C20:0	0.00	0.71	0.84	0.87	0.72	0.00	60.50	59.99	0.00	0.00	0.00
C20:1	0.00	0.77	7.89	0.51	0.44	0.00	0.00	40.01	0.00	0.00	0.00
C20:2	0.00	0.00	0.00	0.00	0.00	0.00	0.00	0.00	0.00	0.00	0.00
C20:3n6	0.00	0.00	0.00	0.00	0.00	0.00	0.00	0.00	0.00	0.00	0.00
C20:4n6	0.00	0.00	0.00	0.00	0.00	0.00	0.00	0.00	0.00	0.00	0.00
C21:0	0.00	0.00	0.00	0.00	0.00	0.00	0.00	0.00	0.00	0.00	0.00
C20:3n3	0.00	0.00	0.76	0.00	0.00	0.00	0.00	0.00	0.00	72.13	0.00
C20:5n3	0.00	0.00	0.00	0.00	0.00	0.00	0.00	0.00	0.00	0.00	0.00
C22:0	0.00	0.73	0.74	0.74	0.56	0.00	0.00	0.00	0.00	0.00	0.00
C22:1n9	0.00	0.23	0.00	0.00	0.00	0.00	0.00	0.00	0.00	0.00	0.00
C22:2	0.00	0.00	0.00	0.00	0.00	0.00	0.00	0.00	0.00	0.00	0.00
C23:0	0.00	3.85	1.99	2.64	1.43	0.00	0.00	0.00	0.00	0.00	0.00
C22:6n3	0.00	0.00	0.00	0.00	0.00	0.00	0.00	0.00	0.00	0.00	0.00
C24:0	0.00	0.45	0.00	0.49	0.37	0.00	0.00	0.00	0.00	0.00	0.00
C24:1	0.00	0.00	0.00	0.00	0.00	0.00	0.00	0.00	0.00	0.00	0.00

G. SEC-MALS-dRI data

This sections contains additional SEC-MALS-dRI data for comparison. Fractions > 0.65 µm not included. Note the wide distributions and lack of adequate separation (complete exclusion) for fractions larger than ~1000kDa. Note the unexpected peak shape of the > 0.65 µm fraction, indicating a cut-off due to the filtration of sample prior to injection. SEC-MALS-dRI data for > 0.65 µm fraction is therefore not included in the dataset.

Fraction	Mw (kDa)	Uncertainty Mw	Rz (nm)	Uncertainty Rz	Conc. from dRI (mg L^{-1})
> 1kDa	35	35 %	-	-	35
> 10 kDa	260	22 %	-	-	48
> 100 kDa	1164	19 %	47	72 %	27
> 1000 kDa	13203	57 %	162	22 %	5
> 0.1 µm	-	-	335	7 %	13
> 0.65 µm	-	-	-	-	-

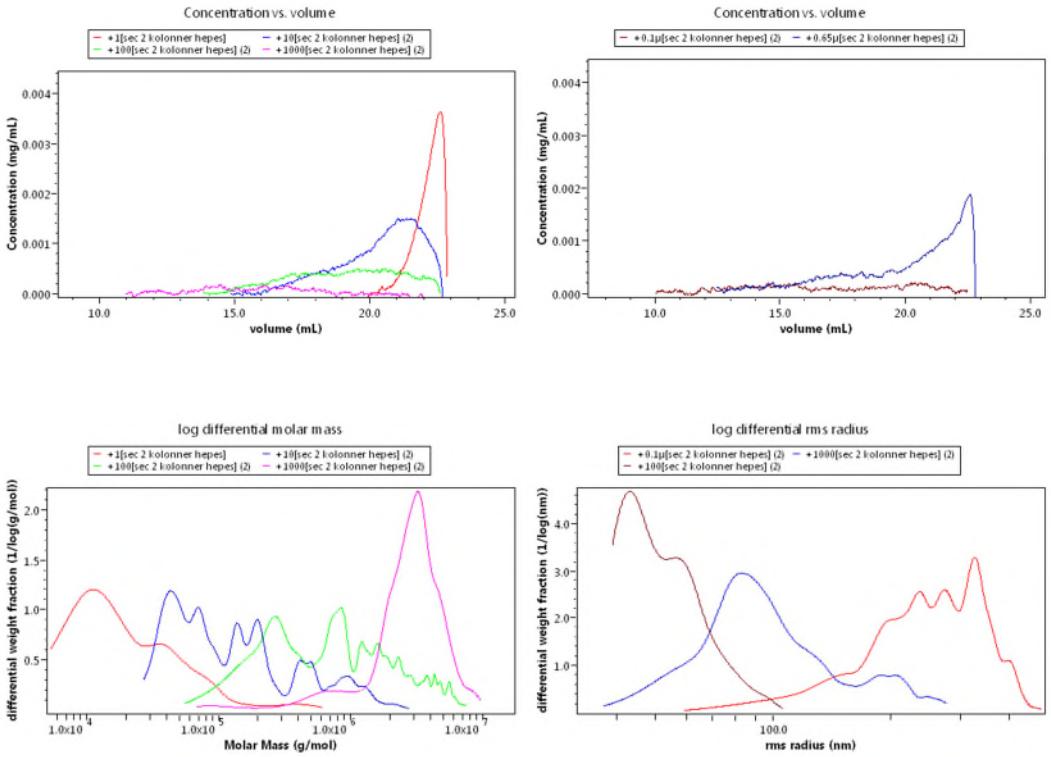

References

Roeleveld, P.J., van Loosdrecht, M.C.M. 2002. Experience with guidelines for wastewater characterisation in The Netherlands. *Water Science and Technology*, **45**(6), 77-87.

Ryckebosch, E., Muylaert, K., Foubert, I. 2012. Optimization of an analytical procedure for extraction of lipids from microalgae. *Journal of the American Oil Chemists' Society*, **89**(2), 189-198.

Wastewater characterisation by combining size fractionation, chemical composition and biodegradability

Ravndal, Kristin T.

2017-12-18

Ravndal K, Opsahl E, Bagi A, Kommedal R, Wastewater characterisation by combining size fractionation, chemical composition and biodegradability, Water Research, Volume 131, 15 March 2018, pp. 151-160

http://doi.org/10.1016/j.watres.2017.12.034